UDC 621.319 https://doi.org/10.20998/2074-272X.2025.2.09

G.V. Bezprozvannych, Y.S. Moskvitin, I.O. Kostiukov, O.M. Grechko

Dielectric parameters of phase and belt paper impregnated insulation of power cables

Introduction. *Medium voltage power cables with paper impregnated insulation remain an important component of power networks. The reliability and efficiency of such cables have been confirmed by their long service life also at nuclear power plants.* ***Problem***. *It is not possible to directly determine the dielectric parameters of phase and belt paper insulation of power cables. Effective electrical diagnostic systems are required to assess the technical condition of such types of power cable insulation. The* ***aim*** *of the work is to substantiate the methodology for determining the dielectric properties of phase and belt paper impregnated insulation based on cumulative measurements of the electrical capacitance and the tangent of the dielectric loss angle of power cables of nuclear power plants and power networks.* ***Methodology***. *The developed methodology is based on the solution of a system of linear algebraic equations of the sixth order for determining the dielectric properties of types of paper impregnated insulation of power three-core cables in a metal sheath.* ***Scientific novelty***. *The differences in the structure of the probing electric field in phase and belt paper insulation depending on the inspection scheme of three-core power cables with sector cores in a metal sheath have been established. The shares of electric energy in the types of insulation under different probing electric field schemes have been determined, which allows determining the tangent of the dielectric loss angle of phase and belt paper insulation.* ***Practical significance***. *The results of the practical implementation of the developed methodology for assessing the differences in the properties of phase and belt insulation of power cables of nuclear power plants and power network cables during spatial scanning of electrical insulation by frequency and voltage, respectively, are presented.* References 41, figures 4, table 6.

Key words: **power cables, aging of paper impregnated insulation, phase and belt insulation, electric field structure, aggregate measurements, commutation matrix, dielectric loss angle tangent, system of linear algebraic equations, self-discharge time constant.**

Вступ. *Силові кабелі середньої напруги з паперовою просоченою ізоляцією залишаються важливою складовою електроенергетичних мереж. Надійність та ефективність таких кабелів підтверджено тривалим терміном експлуатації також на АЕС.* ***Проблема***. *Безпосередньо визначити діелектричні параметри фазної та поясної паперової ізоляції силових кабелів не виявляється можливим. Для оцінки технічного стану таких видів ізоляції силових кабелів необхідні ефективні електричні системи діагностики.* ***Метою*** *роботи є обґрунтування методології визначення діелектричних властивостей фазної та поясної паперової просоченої ізоляції на підставі сукупних вимірювань електричної ємності та тангенсу кута діелектричних втрат силових кабелів АЕС та електричних мереж.* ***Методика***. *Розроблена методика ґрунтується на розв'язанні системи лінійних алгебраїчних рівнянь шостого порядку для визначення діелектричних властивостей видів паперової просоченої ізоляції силових трижильних кабелів у металевій оболонці.* ***Наукова новизна***. *Встановлено відмінності структури зондувального електричного поля у фазній та поясній паперовій ізоляції в залежності від схеми обстеження трижильних силових кабелів із секторними жилами у металевій оболонці. Визначено частки електричної енергії у видах ізоляції за різних схем зондувального електричного поля, що дозволяє визначити тангенс кута діелектричних втрат фазної та поясної паперової ізоляції.* ***Практична значимість***. *Представлено результати практичної реалізації розробленої методики для оцінки відмінностей властивостей фазної та поясної ізоляції силових кабелів АЕС та кабелів енергомереж при просторовому скануванні електричної ізоляції за частотою та напругою відповідно.* Бібл. 41, рис. 4, табл. 6.

Ключові слова: **силові кабелі, старіння паперової просоченої ізоляції, фазна та поясна ізоляція, структура електричного поля, сукупні вимірювання, матриця комутації, тангенс кута діелектричних втрат, система лінійних алгебраїчних рівнянь, стала часу саморозряду.**

Introduction.

Power systems include a significant number of important power cable systems. Paper insulated lead covered cables (PILC) have been used for more than 100 years in medium voltage systems from 6.6 to 36 kV, and even in high voltage systems. Such cable systems have advantages over cross-linked polyethylene cables, primarily in electrical characteristics: high electrical strength, low sensitivity to DC tests and proven operational reliability [1–10].

In modern medium voltage networks, cross-linked polyethylene insulated cables are increasingly used. Replacing paper impregnated cables is a long-term strategy. Paper impregnated cables remain vital components of distribution electrical networks and power systems for circulating pumps in NPP reactor cooling systems [4–7]. It should be noted that the cables have a specified service life of 25 years [7–13]. The actual term is determined by the technical condition of the cable insulation. The physical wear of medium voltage cables with paper impregnated insulation in the power systems of Ukraine is 80 % [7], in European countries it is at the level of 50 %. There are also cables in operation, the service life of which varies from 25 to 60 years. The extension of the service life of nuclear power plants to 60, and even up to 80, years determines the relevance of the problem of assessing the technical condition of cables to ensure reliable and safe operation of power units of stations [7–9].

Problem definition.

During operation, power cables are subject to the complex influence of various factors:

- electric field, which causes electrical aging of the insulation;

- thermal field, which causes thermal aging and oxidation of the insulation;
- wetting of the insulation leads to a deterioration of the electrophysical characteristics of the insulation;
- mechanical aging and damage under the influence of vibration, electrodynamic forces and mechanical loads;
- chemical aging under the influence of aggressive substances [4–13].

Aging of power cable insulation due to prolonged exposure to operational factors can lead to cable breakdown when the limit values of mechanical and electrical insulation characteristics are reached.

Network companies are trying to reduce the frequency of failures and associated costs by monitoring the condition of insulation and maintaining cable systems with paper impregnated insulation. To increase the reliability of power cables and cable lines under operating conditions, various electrical testing and diagnostic methods are used to assess the condition of electrical insulation of power cables, including traditionally used and new modern methods [14–26].

The technical condition of cable insulation is determined by applying constant test voltage that exceeds the nominal by 6 times. Testing cables with an increased test voltage does not allow obtaining reliable information about the real technical condition of power cables with paper impregnated insulation. Such tests of power cables that are operated for a long time often lead to a reduction in service life, untimely and unpredictable insulation breakdown.

Among modern methods, the following non-destructive electrical methods for diagnosing power cables with voltages up to 35 kV inclusive can be distinguished:

- method of measuring partial discharge characteristics [7, 21];
- measurement and analysis of recovery voltage [7, 22–24];
- method of measuring relaxation current (more often in cables with cross-linked polyethylene insulation);
- method of measuring dielectric characteristics of insulation at alternating voltage [23–33].

Measurements at DC voltage allow to detect local defects of the cable line, at AC – to detect general deterioration of the quality of insulation due to its aging.

Unlike short samples of NPP cables – with a length of about 10 m, the examination of which according to electrical characteristics in laboratory conditions can be performed in the frequency range up to 10 kHz [7, 25–27, 34], for long cables of power systems up to 5 km long, it is necessary to conduct an examination at power frequency of 50 (60) Hz to avoid resonance phenomena during the examination and reduce the error in the assessment of diagnostic results.

Power cables with paper impregnated insulation have two types of insulation – phase of each core and belt insulation of three cores together. Insulation is carried out by winding the cores with tapes of cable paper. In the initial state, the properties of the phase and belt insulation must be identical. In the process of cable aging, a synergistic effect of the influence of cable elements and external factors on the aging of paper impregnated insulation is manifested [27, 29, 30, 32].

This causes differences in the mechanical properties of phase and belt insulation, which are caused by the destruction of cellulose and the migration of low-molecular polar products of its decomposition (water, furans) into the colder part of the cable – to the shell, into the belt insulation [23]. As a result, the properties of the belt insulation deteriorate over time to a greater extent compared to the phase insulation. The mechanical strength of cable papers decreases, the dielectric loss tangent increases [7, 15, 27, 30].

It is important to identify signs of aging of each type separately: phase and belt paper electrical insulation, which determines the operability of power cables in operation as an important element of the network. Phase and belt insulation of cables are not available for direct measurements. This causes the averaging of insulation parameters, due to which the differences in their components become less noticeable [25, 27]. As a sign of the end of the period of normal cable operation, differences in the dielectric properties of phase and belt insulation that arise during prolonged operation should be considered. The change in properties can be caused by uneven aging of the specified types of insulation or by moisture due to loss of tightness of connecting and end couplings, protective sheath, etc.

The goal of the work is to substantiate the methodology for determining the dielectric properties of phase and belt paper impregnated insulation based on cumulative measurements of electrical capacitance and dielectric loss tangent of power cables of nuclear power plants and electrical networks.

Structure of the probing electric field in types of paper impregnated insulation of power cables.

The method for determining the dielectric properties of phase and belt paper impregnated insulation is based on establishing differences in the structure of the probing electric field in the type of insulation whose properties are of direct interest.

The density σ of surface electric charges at the interface of the media is found as a result of solving the system of linear algebraic equations (SLAE) in matrix form by the method of secondary sources [25]: Fredholm integral equations of the first kind for potentials on the surfaces of the cores, metal shell and of the second kind for jumps of the normal component of the field strength at the interface of phase and belt electrical insulation, respectively

$$\overline{A} \cdot \overline{\sigma} = \overline{U} , \qquad (1)$$

where $\overline{\sigma}$ is the column matrix of unknown values of the secondary charge density, C/m^2; in nodes of the total number N (order of SLAE), $\overline{U}$ is the column matrix, the first Ne members of which reflect the given potentials of nodes lying on the electrodes, the rest (N – Ne) – on the interface of dielectric media and are equal to zero;

$\overline{A}$ is the square matrix of coefficients, the elements of which a_{ij} are equal to [25]

$$a_{ij}=\left\{\begin{array}{l}\left(\begin{array}{l}\frac{1}{2\pi\varepsilon_0}\ln\frac{r_{0j}}{r_{ij}}\cdot\Delta l_j;\quad \forall i\neq j\\ \frac{1}{2\pi\varepsilon_0}\ln\frac{r_{0j}}{\Delta l_j/(2e)}\cdot\Delta l_j;\quad \forall i=j\end{array}\right) i=1\div N_e\\ \left(\begin{array}{l}\frac{1}{2\varepsilon_0};\quad \forall i=j\\ -\alpha\cdot\frac{1}{2\pi\varepsilon_0}\ln\frac{\cos\left(\overline{r}_{ij},\overline{n}_j\right)}{r_{ij}}\cdot\Delta l_j;\forall i\neq j\end{array}\right) i=N_e+1\div N\end{array}\right\},(2)$$

where i is the node number in which the field characteristics are sought; j is the node number in which the charge is located; r_{ij} is the distance between sections and j; r_{0j} is the distance from section j to point O, the potential of which can be taken to be zero; ε_0 = 8.85·10^{-12} F/m is the electric constant; Δl_j is the length of the segment of the cylinder generator with the center at point j; e is the base of the natural logarithm; α is the parameter associated with the dielectric permittivities of dielectric media: when the normal vector $\overline{n}_j$ is oriented from a medium with a dielectric permittivity ε_2 to a medium with ε_1, the parameter α is equal to:

$$\alpha=\frac{\varepsilon_2-\varepsilon_1}{\varepsilon_2+\varepsilon_1}.$$

During numerical modelling, the coordinates and areas of the sections, the centers of which are nodes located along the thickness of the insulation, are analytically determined, and the boundaries of the cores, phase and belt insulation, and metal sheath are analytically set [25]. The modelling was performed in the open-access software environments Lazarus and Octave.

Figure 1 shows the structure of the electrostatic field (Fig. 1,*a*,*c*,*e*) and the electric field intensity sweeps (Fig. 1,*b*,*d*,*f*) for different schemes of inspection of a power cable in a metal shell for linear voltage of 10 kV with paper impregnated insulation with sector-shaped cores with cross-section of 185 mm^2. The thickness of the phase insulation is 2.75 mm; of the belt insulation is 2 mm. The dielectric permittivity of the phase insulation is ε_1=4.5; of the belt insulation is ε_2=4; in dielectric wedges (in the center and on the periphery) filled with seeping liquid – ε_3=3. The applied phase voltage is 5774 V.

Figures 1,*a*,*c*,*e* show the patterns of electric field strength vectors when the nodes are located on the surface of the electrodes (cores, metal shell), in the thickness of the phase and belt insulation, dielectric wedges for different power cable inspection schemes. Figure 1,*a* corresponds to the cable inspection under the condition of applied electric voltage to one of the cores (*A*) and grounded two others (*B*, *C*) and metal sheath (*S*) – inspection scheme ***I***. Figure 1,*e* – inspection scheme ***II***: electric voltage applied to three cores (*A*, *B*, *C*) and grounded metal shell (*S*).

According to the specified inspection schemes in Fig. 1,*b*,*d*,*f* show the sweeps of the electrostatic field strength at nodes located in the thickness of the phase (*A*, *B*, *C*) and belt (*SA*, *SB*, *SC*) insulation. In the case of inspection scheme ***I***, the electric field is present in the phase and belt insulation (Fig. 1,*a*,*b*). In this scheme, the electrical properties of the phase insulation are more pronounced. The electric charge of the potential core is 2.9 μC/m, of the zero cores is 0.62 μC/m, and of the shell is 1.63 μC/m.

In the case of inspection scheme ***III***, under the condition of electric voltage applied to two cores and the grounded third core and metal shell, the electric field is present in the interphase insulation of the two cores, dielectric wedges, and belt insulation (Fig. 1,*c*,*d*). The electric charge of the potential cores is 2.29 μC/m and 2.29 μC/m, of the zero core is 1.23 μC/m and of the shell is 3.24 μC/m. The identity of the determined values of the electric charges of the two cores proves the high accuracy of the numerical calculations.

With the inspection scheme according to scheme ***II***, the electric field is present to a greater extent in the belt insulation (Fig. 1,*e*,*f*). In the interphase space, the electric field is absent (Fig. 1,*e*) The electric charge of each of the cores is 1.67 μC/m, of the metal shell is 4.98 μC/m.

The results of numerical simulation prove that for any inspection scheme, the electric field enters both the phase and belt insulation (compare Fig. 1,*a*, Fig. 1,*c* and Fig. 1,*e*). At the same time, the grounded cores and the metal shell located nearby significantly affect the value of the electric charge, i.e. the electric capacitance and losses of electric energy in the paper impregnated insulation of the core to which the electric voltage is applied.

Table 1 shows the distribution of the electric field energy (μW) in the phase and belt insulation of the cable determined by the results of numerical calculations for different inspection schemes: scheme ***I*** – «core - against the other two and the metal shell», scheme ***II*** – «three cores together - against the metal sheath».

For each of the selected inspection schemes, the structure of the cable insulation is scanned by an alternating electric field. The electric field is focused in different types of cable insulation: in phase (scheme *A–B*,*C*,*S* – Fig. 1,*a*), belt (scheme *A*,*B*,*C–S* – Fig. 1,*e*) insulation, in the interphase space (scheme *A*,*B – C*,*S* – Fig. 1,*c*).

Depending on the inspection scheme, the electrostatic field energy that accumulates in the types of electrical insulation differs. Thus, according to the scheme «each core against the other two and the shell», the share of energy accumulated in phase insulation is 76.4 %, while in belt insulation only 21.8 % of the total electric field energy in cable insulation is accumulated.

With inspection scheme ***III*** «two cores together – against the third and metal shell», the share of energy in phase insulation is 69.4 %, in belt insulation – 27.4 %. According to scheme ***II***, the share of energy accumulated in phase insulation is 59.4 %, in belt insulation – 43.07 %.

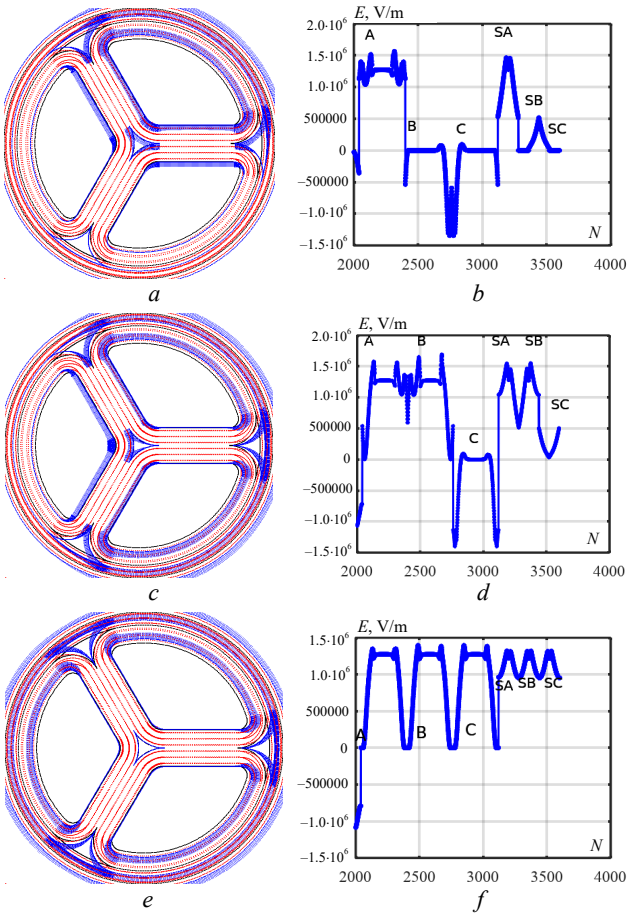

Fig. 1. Structure of the probing electrostatic field in types of paper impregnated electrical insulation under different inspection schemes of a three-core power cable with metal shell

The difference in energy accumulated in different parts of the cable under different schemes of the probing electric field allows to determine the electrical energy losses, i.e. the tangent of the dielectric loss angle directly of the phase and belt insulation. The question is in what way this can be done.

Power cable substitution circuit and methodology for combined capacitance and dielectric loss tangent measurements.

Figure 2 shows the substitution circuit of a three-core power cable in metal shell.

The circuit contains 6 links that reflect the dielectric properties of the insulation of three cores A, B, C to the shell S and between themselves $C_{A\text{-}S}$, $C_{B\text{-}S}$, $C_{C\text{-}S}$, $C_{A\text{-}B}$, $C_{B\text{-}C}$, $C_{C\text{-}A}$, respectively. In parallel with each of the partial capacitances, resistors are included that reflect the dielectric losses in the insulation: $\mathrm{tg}\delta_{A\text{-}S}$, $\mathrm{tg}\delta_{B\text{-}S}$, $\mathrm{tg}\delta_{C\text{-}S}$, $\mathrm{tg}\delta_{A\text{-}B}$, $\mathrm{tg}\delta_{B\text{-}C}$, $\mathrm{tg}\delta_{C\text{-}A}$.

To directly determine partial capacitances with the corresponding losses of electrical energy in insulation (Fig. 2), the method of cumulative measurements of dielectric parameters at alternating voltage of power cables using devices with two terminals is used.

The method of total measurements is more universal than the method of measuring partial capacitance with three terminals. The gap currents, which are discharged to the ground using the third terminal past the measuring circuit, affect the measurement results of the selected one. The error of the measurement results with three terminals can be significant, especially in operation [35].

Table 1

Electrostatic field energy shares in electrical insulation components depending on the inspection scheme of 10 kV power cable

Type of insulation	Inspection scheme					
	Scheme ***I***: «core A – against grounded cores B, C and metal shell S» applied voltage U=5774 V		Scheme ***III***: «cores A, B – against grounded core C and metal shell S» applied voltage U=5774 V		Scheme ***II***: «cores A, B, C – against grounded metal shell S» applied voltage U=5774 V	
	W_A, mJ/m	The share of energy stored in the type of insulation $\eta_A = W_A/W$	$W_{A,B}$, mJ/m	The share of energy stored in the type of insulation $\eta_{A,B} = W_{A,B}/W$	$W_{A,B,C}$, mJ/m	The share of energy stored in the type of insulation $\eta_{A,B,C} = W_{A,B,C}/W$
Phase insulation of the core A	4,73	0,5761	3,66	0,28	2,74	0,198
Phase insulation of the core B	0,81	0,099	3,70	0,28	2,76	0,198
Phase insulation of the core C	0,81	0,099	1,75	0,134	2,76	0,198
Belt insulation between the cores and shell	1,79	0,218	3,58	0,274	5,62	0,4307
Belt insulation between core C and shell	0,0453	0,0052	0,045	0,0034	0	0
Interphase insulation between cores C and A	0,1181	0,0144	0,0996	0,0077	0,0107	0,00082
Interphase insulation between cores C and B	$3{,}074\cdot10^{-9}$	0	0,1125	0,0086	0,0109	0,00083
Interphase insulation between cores A and B	0,1217	0,0148	0,1135	0,0087	0,0110	0,00084
Total energy W, mJ/m	8,21	1	13,071	1	13,913	1

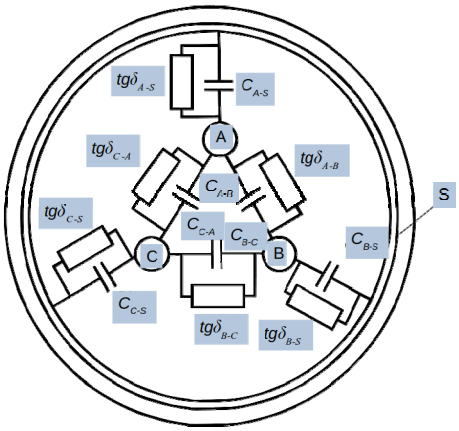

Fig. 2. Substitution circuit of a three-core power cable in a metal shell

The dielectric parameters of the controlled circuit are not found directly during the measurements, but as a result of solving the SLAE. The method can be implemented both using devices with three terminals (in this case, one terminal is not used) and using devices with two terminals. A two-position switch (*C*, Fig. 3) is placed between the object and the meter.

Each of the terminals of the three-core (*A*, *B*, *C*) power cable in a metal shell (*S*) is connected to one (*i*) or the other (*j*) input of the device (I).

The scheme of inspection of a three-core power cable with paper impregnated insulation in a metal shell using the method of cumulative measurements is presented in Fig. 3.

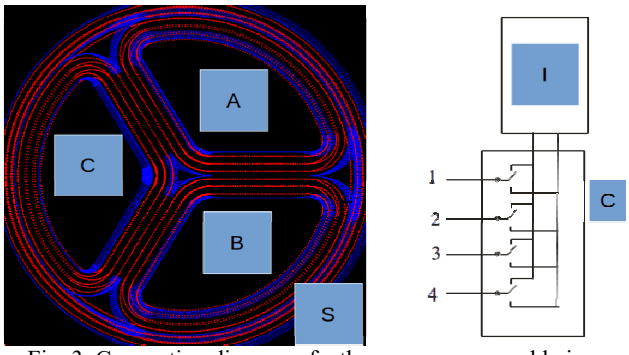

Fig. 3. Connection diagram of a three-core power cable in a metal shell to a two-position switch

In a three-core cable with a metal shell, 7 complete inspection schemes can be distinguished by the method of cumulative measurements for monitoring the electrical capacitance and dielectric loss tangent of the power cable.

Four schemes reflect the dielectric properties of the phase and belt insulation between the cores and the metal sheath for the cases: according to scheme ***I*** «each of the three cores – against the grounded two others and the metal shell» (Fig. 1,*a*) and according to scheme ***II*** «all three cores together – against the grounded metal shell» (Fig. 1,*e*). The corresponding total electrical capacitances $C_{A\text{-}B,C,S}$, $C_{B\text{-}A,C,S}$, $C_{C\text{-}A,B,S}$, $C_{A,B,C\text{-}S}$ and the total dielectric loss tangents $\text{tg}\delta_{A\text{-}B,C,S}$, $\text{tg}\delta_{B\text{-}A,C,S}$, $\text{tg}\delta_{C\text{-}A,B,S}$, $\text{tg}\delta_{A,B,C\text{-}S}$ are recorded.

Three inspection schemes ***III*** reflect the dielectric properties of the interphase insulation (Fig. 1,*c*). In this case, the device records the corresponding total electrical capacitances and total dielectric loss tangents: $C_{A,B\text{-}C,S}$, $C_{C,A\text{-}B,S}$, $C_{B,C\text{-}A,S}$, $\text{tg}\delta_{A,B\text{-}C,S}$, $\text{tg}\delta_{C,A\text{-}B,S}$, $\text{tg}\delta_{B,C\text{-}A,S}$.

The state of the switch keys is determined by the switching matrix *AK*, the elements of which are equal to «1» in the case of connecting the object terminal, for example, to the left terminal of the device and «0» in the opposite case – to the right (Fig. 3):

$$AK=\begin{bmatrix} 0&1&0&1&0&1&0&1&0&1&0&1&0&1&0&1\\ 0&0&1&1&0&0&1&1&0&0&1&1&0&0&1&1\\ 0&0&0&0&1&1&1&1&0&0&0&0&1&1&1&1\\ 0&0&0&0&0&0&0&0&1&1&1&1&1&1&1&1 \end{bmatrix}. \quad (3)$$

The matrix contains 4 rows (by the number of terminals of the control object) and 2^4=16 columns (by the number of all possible options for the state of the switch keys). The first and last columns correspond to degenerate cases: 0000 – all poles of the object are connected to one terminal, and 1111 – to the other terminal of the meter. These experiments can be used to estimate the parasitic capacitance of the switch and connecting wires. The other experiments (there are a total of *Ne*=16 – 2 = 14) are divided into two groups. The first 7 experiments are the main ones (columns (2 – 8) in (3)), the others are inverse (columns (9–15) – correspond to a change in the polarity of the connection to all poles).

The unknown partial capacities are found based on the results of cumulative measurements from the SLAE:

$$AC\times Cx = Ce, \quad (4)$$

where *Ce* is the column matrix of the results of the cumulative measurements: $C_{A\text{-}B,C,S}$, $C_{B\text{-}A,C,S}$, $C_{C\text{-}A,B,S}$, $C_{A,B,C\text{-}S}$, $C_{A,B\text{-}C,S}$, $C_{C,A\text{-}B,S}$, $C_{B,C\text{-}A,S}$; *Cx* is the column matrix of unknown partial capacitances: $C_{A\text{-}B}$, $C_{B\text{-}C}$, $C_{C\text{-}A}$, $C_{A\text{-}S}$, $C_{B\text{-}S}$, $C_{C\text{-}S}$); *AC* is the matrix of the «participation» of the partial capacitance in the total capacitance for this experiment.

Element a_{ij} of the matrix *AC* is equal to 1 if the difference of the codes of poles *i* and *j* is different from zero, and is equal to 0 otherwise.

In experiment 2 (second column in (3): the first terminal «1», the rest are zero) the capacitances connected in parallel are measured: $C_{A\text{-}B} + C_{C\text{-}A} + C_{A\text{-}S}$. In experiment 3 (third column in (3): second terminal «1», the rest are zero) the capacitances connected in parallel are measured: $C_{A\text{-}B} + C_{B\text{-}C} + C_{B\text{-}S}$.

The partial capacitances that participate in the total capacitance for a particular experiment are found by multiplying the row of the matrix *AC* by the column matrix *Cx*:

$$AC\times Cx=\begin{bmatrix} 1&1&0&1&0&0\\ 1&0&1&0&1&0\\ 0&1&1&1&1&0\\ 0&1&1&0&0&1\\ 1&0&1&1&0&1\\ 1&1&0&0&1&1\\ 0&0&0&1&1&1 \end{bmatrix}\times\begin{bmatrix} C_{A-B}\\ C_{B-C}\\ C_{C-A}\\ C_{A-S}\\ C_{B-S}\\ C_{C-S} \end{bmatrix}.$$

The SLAE, similar to (4), is also written to find tgδ of partial capacitances:

$$ATG \times TGx = TGe, \quad (5)$$

where TGe is the column matrix of measured total values of tgδ (the result of the total action of a number of partial capacitances with losses connected in parallel); TGx is the column matrix of values of tgδ of the partial capacitance with losses, which is **the purpose of the calculation**; ATG is the matrix of coefficients, similar in structure to the AC matrix, but instead of unit coefficients, contains fractions, in the numerator of which are the partial capacitances C_{ij}, found as a result of solving (4), and in the denominator – the sums of the partial capacitances participating in this experiment.

The coefficients of the ATG matrix determine the shares of the real values of the partial capacitances (with electrical energy losses) in the total losses for this experiment.

When implementing all 7 basic experiments according to (4), (5), the SLAE becomes overdetermined: the number of equations is greater than the number of unknowns [25]. Finding the solution requires the application of the least squares method:

$$Cx = (AC' \times AC)^{-1} \times AC' \times Ce, \quad (6)$$

where «′« means transposition; degree «–1» – finding the inverse matrix; sign «×« – matrix multiplication.

Similarly, the unknown values of the tangents of the angle of dielectric losses of partial capacitances are found, which is **the purpose of the study**:

$$TGx = (ATG' \times ATG)^{-1} \times ATG' \times TGe. \quad (6)$$

To find the dielectric parameters of phase and belt insulation, it is enough to perform 6 experiments out of the 7 main ones, for example: 2 – 7: $C_{A\text{-}B,C,S}$, $C_{B\text{-}A,C,S}$, $C_{C\text{-}A,B,S}$, $C_{A,B,C\text{-}S}$, $C_{A,B\text{-}C,S}$, $C_{C,A\text{-}B,S}$.

When implementing 6 experiments (columns (2–7) of the commutation matrix AK (3)), we obtain a 6th-order SLAE with the matrix AC of the form:

$$AC = \begin{bmatrix} 1 & 1 & 0 & 1 & 0 & 0 \\ 1 & 0 & 1 & 0 & 1 & 0 \\ 0 & 1 & 1 & 1 & 1 & 0 \\ 0 & 1 & 1 & 0 & 0 & 1 \\ 1 & 0 & 1 & 1 & 0 & 1 \\ 1 & 1 & 0 & 0 & 1 & 1 \end{bmatrix}.$$

The corresponding inverse matrix AC^{-1} is:

$$AC^{-1} = 0{,}5 \times \begin{bmatrix} 1 & 1 & -1 & 0 & 0 & 0 \\ 1 & 0 & 0 & 1 & -1 & 0 \\ 0 & 1 & 0 & 1 & 0 & -1 \\ 0 & -1 & 1 & -1 & 1 & 0 \\ -1 & 0 & 1 & -1 & 0 & 0 \\ -1 & -1 & 0 & 0 & 1 & 1 \end{bmatrix}.$$

The sought partial capacitances are found by multiplying the rows of the inverse matrix by the column of experimental data.

For example, the first unknown capacitance $C_{A\text{-}B}$ is found by multiplying the first row of the matrix AC^{-1} by the column of measurement results (8). This provides grounds to determine tg$\delta_{A\text{-}B}$ by (9), where $C_{A\text{-}B,C,S}$, $C_{B\text{-}A,C,S}$, $C_{C\text{-}A,B,S}$, $C_{A,B,C\text{-}S}$, $C_{A,B\text{-}C,S}$, $C_{C,A\text{-}B,S}$ are the experimental results of the combined measurements, the sequence of which is given by columns (2–7) of the switching matrix (1), $C_{s1} = C_{A\text{-}B,C,S} + C_{B\text{-}A,C,S} + C_{C\text{-}A,B,S}$ is the total electrical capacitance of the experiment, which corresponds to the first row of the matrix AC.

Note that formula (9) can be used only after the partial capacitances $C_{A\text{-}B}$, $C_{B\text{-}C}$, C_{CA} are found.

The formulas for the parameters of other partial capacitances and dielectric loss tangents are determined according to (8), (9):

$$C_{A-B} = 0{,}5(C_{A-B,C,S} + C_{B-A,C,S} - C_{C-A,B,S} + 0 \times C_{A,B,C-S} + 0 \times C_{A,B-C,S} + 0 \times C_{C,A-B,S}); \quad (8)$$

$$\mathrm{tg}\delta_{A-B} = 0{,}5 \times \left(\frac{C_{A-B}}{C_{s1}} \mathrm{tg}\delta_{A-B,C,S} + \frac{C_{B-C}}{C_{s1}} \mathrm{tg}\delta_{B-A,C,S} - \frac{C_{C-A}}{C_{s1}} \mathrm{tg}\delta_{C-A,B,S} + 0 \times \mathrm{tg}\delta_{A,B,C-S} + 0 \times \mathrm{tg}\delta_{A-B-C,S} + 0 \times \mathrm{tg}\delta_{CA-B,S} \right). \quad (9)$$

Thus, the solution of SLAE (4) and (5) in practice is reduced to formulas that are linear combinations of measurement results taken with certain weighting factors. Calculation using them does not present any particular difficulties.

To determine the dielectric parameters of phase and belt insulation based on the method of cumulative measurements, a spatial method of creating a probing electric field in the type of paper impregnated insulation of power cables, the properties of which must be determined, is used. For this purpose, the conductors and metal shell of the power cable are switched in a way that shunts the electric field in those parts of the structure, the influence of which must be neglected.

In the case of implementing the specified method for short samples of power cables of NPPs, it is possible to conduct an examination at several values of the frequency of the sound range 0.1–10 kHz of low voltage to determine the predominant factors of the aging process over time of phase and belt paper impregnated insulation. For long-distance cables, for example, urban power networks, the use of the frequency method is limited to one power operating frequency at several values of high applied voltage. Examination of cables in operation at several values of frequency is limited by resonance phenomena between the cable's own inductance and capacitance.

Examples of practical implementation of the methodology for determining the dielectric properties of phase and belt paper impregnated insulation of power cables.

Figure 4 shows the general and determined on the basis of the proposed methodology electrical characteristics of types of electrical insulation in the form of C-tgδ diagrams for frequencies of 0.1; 1 and 10 kHz of samples of power cables of nuclear power plants for voltage of 6 kV with paper impregnated insulation in laboratory conditions. The designation of experimental data corresponds to frequencies of 0.1; 1 and 10 kHz: the total measurement results – red, green and blue colors;

determined dielectric parameters of phase and belt insulation – purple, turquoise and black colors, respectively.

For the cable sample (Fig. 4,*a*), higher values of tgδ of phase and belt insulation are observed for a frequency of 0.1 kHz, which is evidence of moistening of paper impregnated insulation during long-term operation. At the same time, belt insulation is more aged compared to phase one: tgδ values differ by more than 1.33 times for frequency of 10 kHz.

For the cable sample (Fig. 4,*b*), lower values of dielectric losses of phase and belt insulation are observed for frequency of 100 Hz. This is evidence of a lower moisture content in the insulation under the influence of the increased operating temperature of the cable during operation. At the same time, for frequency of 10 kHz, the belt insulation is also characterized by 25 % higher tgδ values compared to the phase insulation.

In any case, changing the inspection scheme leads to significant variations in tgδ, which is a sign of aging of the paper impregnated cable insulation (Fig. 4).

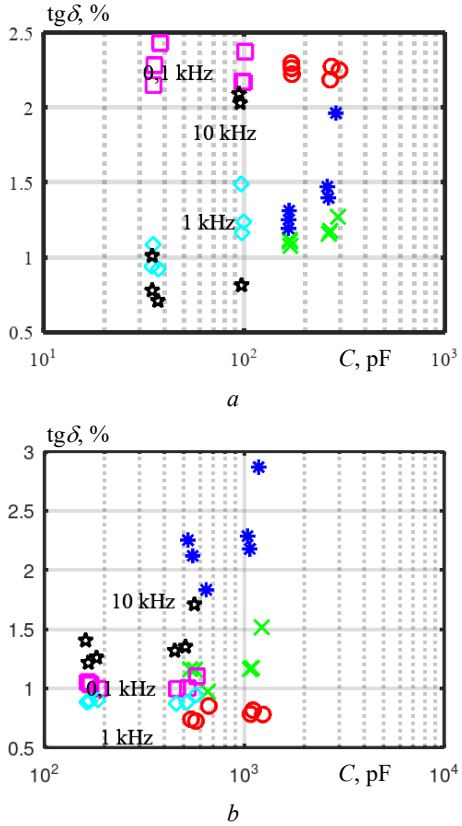

Fig. 4. Dielectric parameters of paper impregnated electrical insulation of NPP cable samples for different frequency values

Table 2–5 present the determined dielectric parameters based on the results of combined measurements of cables directly in operation of 10 kV power cable lines.

Thus, the belt insulation of phases *A*, *B* and *C* of cables (Table 2, 3) has practically the same values.

This, firstly, indirectly indicates a uniform current load during long-term operation. Secondly, the values of tgδ remain practically unchanged with an increase in the applied test voltage: the absence of air cavities. Electrical energy losses due to ionization are not observed (evidence of the uniformity of filling of dielectric wedges with an impregnating compound – Fig. 1).

Table 2

Dielectric parameters of phase and belt insulation of the AASHV-3×120 cable for voltage of 10 kV, length 240 m

Inspection scheme	Applied voltage					
	2 kV		5 kV		8 kV	
	C, nF	tgδ, %	*C*, nF	tgδ, %	*C*, nF	tgδ, %
A-S	47,9738	0,3456	49,2300	0,3475	48,6638	0,3308
B-S	48,4738	0,3376	47,8800	0,3503	48,4937	0,3348
C-S	48,7237	0,3280	48,8800	0,3334	49,0638	0,3441
A-B	12,0725	0,1802	12,0400	0,1146	12,1625	0,1318
B-C	12,4225	0,2492	12,8800	0,1799	12,1925	0,1488
C-A	12,4825	0,2202	12,0400	0,1396	12,4125	0,1418

Table 3

Dielectric parameters of phase and belt insulation of the AASHV-3×70 cable for voltage of 10 kV, length 220 m

Inspection scheme	Applied voltage					
	2 kV		5 kV		8 kV	
	C, nF	tgδ, %	*C*, nF	tgδ, %	*C*, nF	tgδ, %
A-S	29,86	0,666	29,9266	0,7265	29,9913	0,7204
B-S	29,63	0,655	29,5876	0,6312	29,5913	0,6346
C-S	29,85	0,624	29,7946	0,6534	29,7912	0,6653
A-B	7,491	0,108	7,4657	0,1311	7,3975	0,1305
B-C	7,361	0,097	7,4578	0,1211	7,4975	0,1157
C-A	7,471	0,112	7,449	0,1261	7,476	0,126

Table 4

Dielectric parameters of phase and belt insulation of cable AASHV-3×120 for voltage 10 kV, length 2470 m

a) before repair – phase *C* damaged

Inspection scheme	Applied voltage					
	2 kV		5 kV		8 kV	
	C, nF	tgδ, %	*C*, nF	tgδ, %	*C*, nF	tgδ, %
A-S	636,3	1,00	616,5	0,891	840,1	1,39
B-S	639,9	0,99	618,4	0,896	839	1,61
C-S	phase *C* damaged					
A-B	99,48	1,842	119	2,151	97,69	1,203
B-C	97,5	1,346	99,3	1,802	119,3	2,158
C-A	phase *C* damaged					

b) after repair

Inspection scheme	Applied voltage					
	2 kV		5 kV		8 kV	
	C, nF	tgδ, %	*C*, nF	tgδ, %	*C*, nF	tgδ, %
A-S	500,756	0,7640	501,062	0,8341	504,2875	0,8624
B-S	498,256	0,7774	498,162	0,8511	502,1875	0,8570
C-S	497,756	0,7600	497,462	0,8582	501,5875	0,8830
A-B	139,937	0,7164	139,675	0,7202	138,5250	0,7212
B-C	141,637	0,7252	141,475	0,7202	140,1250	0,7442
C-A	141,637	0,7452	141,475	0,7242	140,3250	0,7242

Table 5

Dielectric parameters of phase and belt insulation of the AASHV-3×95 cable for voltage of 10 kV, length 40 m

Inspection scheme	Applied voltage					
	2 kV		5 kV		8 kV	
	C, nF	tgδ, %	C, nF	tgδ, %	C, nF	tgδ, %
A-S	12,6340	0,6654	12,7731	0,7312	12,4834	0,7503
B-S	12,5230	0,6673	12,3241	0,8482	12,7184	0,7772
C-S	12,9240	1,7844	13,1081	1,8594	12,8934	1,7415
A-B	3,1630	0,3537	3,1978	0,0778	3,1433	0,1053
B-C	3,2130	0,3446	3,3227	0,0938	3,1332	0,1233
C-A	3,1620	0,2077	2,8337	0,1030	3,3583	0,0982

After repair of the damaged phase C of the power cable AASHV-3×120 (Table 4), the uniformity of aging of the belt and phase insulation of all three phases was established. After repair, the tgδ level decreased, but remained in the range from 0.6 to 0.8 %, which corresponds to moderately aged insulation [29].

The AASHV-3×95 cable (Table 5) is characterized by non-uniform current load in operation. As a result, the insulation of phase *C* has 2.3 times higher tgδ values: it is significantly aged compared to the others. The critical tgδ values for the frequency of 50 Hz correspond to the critical value of mechanical strength by the number of double bends of cable papers and have the following values: for phase insulation: 1.2673–1.3874 %; for belt insulation: 1.29–1.4886 % [36]. Additional direct current inspections in operation proved the defectiveness of the cable coupling of phase *C*.

Measurements at direct voltage allow to detect local defects of the cable line – leakage of impregnating liquid, which most often occur in connecting and end couplings [37–40].

Measurement of leakage current at direct current when applying a voltage of 40 kV allowed to determine the insulation resistance Ris of phase C of the cable line with the coupling. The product of the insulation resistance R_{is} and the electrical capacitance of phase *C* (Table 5, *C-S* = 12.924 nF) determines the self-discharge time constant of the insulation $\theta = R_{is} \cdot C$ – an objective indicator of quality that does not depend on the geometric dimensions of the insulation.

Thus, the signs of defects in elements of cable lines with paper impregnated insulation are established on the basis of the ratio of the values of tgδ of the types of cable insulation (the result of measurements on AC) and the self-discharge time constant (the result of measurements on direct current of insulation resistance and electric capacitance on AC) (Table 6).

Table 6

Classification of defects in cable lines with paper impregnated insulation [41]

Value range of θ, s	tgδ < (0,5 – 1) %	tgδ > (1 – 2) %
θ < (1 – 10)	Coupling	Coupling and cable
θ > (10 – 100)	Normal state	Cable

In the considered case, the self-discharge time constant of phase *C* is θ = 1.52 s; for phases *A* and *B*: θ = 12.14 s and 7.43 s, respectively.

Conclusions.

1. The established differences in the structure of the probing electric field in the types of paper impregnated electrical insulation made it possible to determine the share of energy accumulated in the phase, belt insulation and interphase space in the cable as a whole.

2. It has been proven that according to the inspection schemes «each of the three cores – against the grounded two others and the metal shell» and «three cores together – against the grounded shell», the probing electric field is concentrated mainly in the phase or belt insulation of the cable, respectively. This provided the basis for developing a methodology for determining the dielectric parameters of the types of electrical insulation – phase and belt insulation of power cables.

3. The methodology is based on solving a system of linear algebraic equations of the 6th order, which reflects the results of six cumulative measurements of the dielectric parameters of three-core power cables in a metal shell.

4. The results of the practical implementation of the developed methodology for assessing the differences in the properties of phase and belt insulation of NPP power cables and power network cables are presented.

5. The need to compare the results of diagnostic examinations on direct and alternating currents to increase the accuracy of assessing the technical condition of power cables with paper impregnated insulation in operation is argued.

Conflict of interest. The authors of the article declare no conflict of interest.

REFERENCES

1. Zapf M., Blenk T., Müller A.-C., Pengg H., Mladenovic I., Weindl C. Lifetime Assessment of PILC Cables with Regard to Thermal Aging Based on a Medium Voltage Distribution Network Benchmark and Representative Load Scenarios in the Course of the Expansion of Distributed Energy Resources. *Energies*, 2021, vol. 14, no. 2, art. no. 494. doi: https://doi.org/10.3390/en14020494.

2. *Assessing and Managing Cable Ageing in Nuclear Power Plants*. IAEA Nuclear Energy Series, No. NP-T-3.6. Vienna, IAEA, 2012. 96 p.

3. Šimić Z., Peinador Veira M., Banov R. Correlation between events with different safety significance in nuclear power plants. *Nuclear Engineering and Technology*, 2022, vol. 54, no. 7, pp. 2510-2518. doi: https://doi.org/10.1016/j.net.2022.01.034.

4. Hettal S., Suraci S.V., Roland S., Fabiani D., Colin X. Towards a Kinetic Modeling of the Changes in the Electrical Properties of Cable Insulation during Radio-Thermal Ageing in Nuclear Power Plants. Application to Silane-Crosslinked Polyethylene. *Polymers*, 2021, vol. 13, no. 24, art. no. 4427. doi: https://doi.org/10.3390/polym13244427.

5. *Ageing Management for Nuclear Power Plants: International Generic Ageing Lessons Learned (IGALL)*. IAEA Safety Reports Series, no. 82 (rev. 1). Vienna, IAEA, 2020. 120 p.

6. *Equipment Qualification for Nuclear Installations*. IAEA Specific Safety Guides, no. SSG-69, Vienna, 2021. 53 p.

7. Bezprozvannych G., Moskvitin Y. Aging management of cables of nuclear power plants. *Energy Saving. Power Engineering. Energy Audit*, 2022, no. 11-12 (177-178), pp. 21-33. (Ukr). doi: https://doi.org/10.20998/2313-8890.2022.11.02.

8. Mazzanti G., Montanari G.C., Dissado L.A. Electrical aging and life models: the role of space charge. *IEEE Transactions on*

Dielectrics and Electrical Insulation, 2005, vol. 12, no. 5, pp. 876-890. doi: https://doi.org/10.1109/TDEI.2005.1522183.
9. *Cable ageing in nuclear power plants report on the first and second terms (2012-2017) of the NEA cable ageing data and knowledge (CADAK) project*. Vienna, IAEA, 2018. 60 p.
10. Shaalan E.M., Ward S.A., Youssef A. Analysis of a Practical Study for Under-Ground Cable Faults Causes. *2021 22nd International Middle East Power Systems Conference (MEPCON)*, 2021, vol. 208-215. doi: https://doi.org/10.1109/MEPCON50283.2021.9686288.
11. Klimenta J., Panic M., Stojanovic M., Klimenta D., Milovanovic M., Perovic B. Thermal aging management for electricity distribution networks: FEM-based qualification of underground power cables. *Thermal Science*, 2022, vol. 26, no. 4 Part B, pp. 3571-3586. doi: https://doi.org/10.2298/TSCI220128050K.
12. Mustafa E., Afia R.S.A., Nouini O., Tamus Z.A. Implementation of Non-Destructive Electrical Condition Monitoring Techniques on Low-Voltage Nuclear Cables: I. Irradiation Aging of EPR/CSPE Cables. *Energies*, 2021, vol. 14, no. 16, art. no. 5139. doi: https://doi.org/10.3390/en14165139.
13. Kim J., Kim W., Park H.-S., Kang J.-W. Lifetime Assessment for Oil-Paper Insulation using Thermal and Electrical Multiple Degradation. *Journal of Electrical Engineering and Technology*, 2017, vol. 12, no. 2, pp. 840-845. doi: https://doi.org/10.5370/JEET.2017.12.2.840.
14. Mladenovic I., Weindl C. Artificial aging and diagnostic measurements on medium-voltage, paper-insulated, lead-covered cables. *IEEE Electrical Insulation Magazine*, 2012, vol. 28, no. 1, pp. 20-26. doi: https://doi.org/10.1109/MEI.2012.6130528.
15. Carrascal I.A., Fernández-Diego C., Casado J.A., Diego S., Fernández I., Ortiz A. Quantification of Kraft paper ageing in mineral oil impregnated insulation systems through mechanical characterization. *Cellulose*, 2018, vol. 25, no. 6, pp. 3583-3594. doi: https://doi.org/10.1007/s10570-018-1788-1.
16. Bezprozvannych G.V., Moskvitin Y.S. Physical Processes of Aging and Assessment of the Technical Condition of Power Cables with Paper-Impregnated Insulation. *2023 IEEE 4th KhPI Week on Advanced Technology (KhPIWeek)*, 2023, pp. 1-5. doi: https://doi.org/10.1109/KhPIWeek61412.2023.10312975.
17. Basu D., Gholizad B., Ross R., Gargari S.M. Thermal Aging-Based Degradation Parameters Determination for Grid-Aged Oil Paper Insulation. *IEEE Transactions on Dielectrics and Electrical Insulation*, 2023, vol. 30, no. 2, pp. 734-743. doi: https://doi.org/10.1109/TDEI.2022.3217434.
18. Kiger C.J., Hashemian H.M., Sexton C.D., Toll T.A. Research gap in management of insulation aging of medium voltage cables in nuclear power plants. *Transactions of the American Nuclear Society*, 2018, vol. 118, no. 1, pp. 593-594.
19. Kim J-S., Lee D.-J. Evaluation of nuclear plant cable aging through condition monitoring. *Nuclear Engineering and Technology*. 2004, vol. 36, no. 5, pp. 474-475.
20. Fabiani D., Suraci S.V., Bulzaga S. Aging Investigation of Low-Voltage Cable Insulation Used in Nuclear Power Plants. *2018 IEEE Electrical Insulation Conference (EIC)*, 2018, pp. 516-519. doi: https://doi.org/10.1109/EIC.2018.8481139.
21. Shafiq M., Kauhaniemi K., Robles G., Isa M., Kumpulainen L. Online condition monitoring of MV cable feeders using Rogowski coil sensors for PD measurements. *Electric Power Systems Research*, 2019, vol. 167, pp. 150-162. doi: https://doi.org/10.1016/j.epsr.2018.10.038.
22. Bezprozvannych G.V., Kostukov I.O., Moskvitin E.S. Differentiation of absorption processes in inhomogeneous insulation by curve of recovering voltage of power high voltage cables. *Technical electrodynamics*, 2021, no. 6, pp. 13-19. (Ukr). doi: https://doi.org/10.15407/techned2021.06.013.
23. Kyrylenko V.M., Kyrylenko K.V., Budko M.O., Denysiuk P.L. Reasoning of additional diagnostic parameters for electric insulation diagnostics by absorption methods. *Electrical Engineering & Electromechanics*, 2021, no. 6, pp. 39-45. doi: https://doi.org/10.20998/2074-272X.2021.6.06.
24. Bezprozvannych G.V., Moskvitin E.S., Kyessayev A.G. The absorption characteristics of the phase and zone paper-impregnated insulation of power cable at direct voltage. *Electrical Engineering & Electromechanics*, 2015, no. 5, pp. 63-68. (Rus). doi: https://doi.org/10.20998/2074-272X.2015.5.09.
25. Bezprozvannych G.V., Rudakov S.V., Moskvitin E.S. *Prevention of emergency situations by monitoring the state of insulation of multi-core cables according to the parameters of partial capacitances and tangent of dielectric losses*. *Monograph*. Kharkiv, 2013. 165 p. (Rus).
26. Kostiukov I. Measurement of Dissipation Factor of Inner Layers of Insulation in Three-Core Belted Cables. *Lighting Engineering & Power Engineering*, 2021, vol. 60, no. 1, pp. 23-30. doi: https://doi.org/10.33042/2079-424X.2021.60.1.04.
27. Cherukupalli S., Buchholz V., Colwell M., Crine J.-P., Keefe R.J. Condition assessment of distribution PILC cables from electrical, chemical, and dielectric measurements. *IEEE Electrical Insulation Magazine*, 2004, vol. 20, no. 4, pp. 6-12. doi: https://doi.org/10.1109/MEI.2004.1318834.
28. Cichecki P., Gulski E., Smit J.J., van Nes P., Ejigu A.G., de Vries F. Dielectric losses diagnosis of serviced aged oil impregnated paper insulation of HV power cables. *2009 IEEE Electrical Insulation Conference*, 2009, pp. 216-219. doi: https://doi.org/10.1109/EIC.2009.5166348.
29. Kim S.-J., Lee S., Choi W.-S., Lee B.-W. Experimental and Simulation Studies on Stable Polarity Reversal in Aged HVDC Mass-Impregnated Cables. *Energies*, 2024, vol. 17, no. 10, art. no. 2352. doi: https://doi.org/10.3390/en17102352.
30. Florkowski M., Kuniewski M., Mikrut P. Effects of mechanical transversal bending of power cable on partial discharges and dielectric-loss evolution. *IEEE Transactions on Dielectrics and Electrical Insulation*, 2024, pp. 1-1. doi: https://doi.org/10.1109/TDEI.2024.3382642.
31. Rowland S., Wang M. Fault Development in Wet, Low Voltage, Oil-Impregnated Paper Insulated Cables. *IEEE Transactions on Dielectrics and Electrical Insulation*, 2008, vol. 15, no. 2, pp. 484-491. doi: https://doi.org/10.1109/TDEI.2008.4483468.
32. Hakonseth G., Ildstad E., Furuheim K.M. Local Electric Field in Mass-Impregnated HVDC Cables. *Proceedings of the Nordic Insulation Symposium*, 2017, no. 25. doi: https://doi.org/10.5324/nordis.v0i25.2351.
33. Borghetto J., Pirovano G., Tornelli C., Contin A. Frequency Dielectric Spectroscopy and Dissipation Factor Measurements during Thermal Cycles on Different Types of MV Cable Joints. *2021 IEEE Electrical Insulation Conference (EIC)*, 2021, pp. 441-446. doi: https://doi.org/10.1109/EIC49891.2021.9611379.
34. Besprozvannych A.V., Naboka B.G., Moskvitin E.S. Inspection of the insulation of three-phase cables in a metal sheath. *Electricity*, 2010, no. 1, pp. 48-54. (Rus).
35. Besprozvannych A.V., Naboka B.G. The influence of parasitic capacitances on the results of measurements of parameters of multi-core cables when assessing their technical condition. *Electricity*, 2011, no. 5, pp. 27-36. (Rus).
36. Bezprozvannych G.V., Moskvitin E.S. Estimation criteria for degree of paper-impregnated insulated power cable ageing. *Electrical Engineering & Electromechanics*, 2013, no. 4, pp. 32-36. (Rus).
37. Su J., Wei L., Zhang P., Li Y., Liu Y. Multi-type defect detection and location based on non-destructive impedance

spectrum measurement for underground power cables. *High Voltage*, 2023, vol. 8, no. 5, pp. 977-985. doi: https://doi.org/10.1049/hve2.12331.

38. Neimanis R., Eriksson R., Papazyan R. Diagnosis of Moisture in Oil/Paper Distribution Cables – Part II: Water Penetration in Cable Insulation–Experiment and Modeling. *IEEE Transactions on Power Delivery*, 2004, vol. 19, no. 1, pp. 15-20. doi: https://doi.org/10.1109/TPWRD.2003.820430.

39. Neimanis R., Eriksson R. Diagnosis of Moisture in Oil/Paper Distribution Cables – Part I: Estimation of Moisture Content Using Frequency-Domain Spectroscopy. *IEEE Transactions on Power Delivery*, 2004, vol. 19, no. 1, pp. 9-14. doi: https://doi.org/10.1109/TPWRD.2003.820417.

40. Bonanno R., Lacavalla M. A feasibility analysis aimed at defining an alert system for Distribution MV Underground Cables. *2020 AEIT International Annual Conference (AEIT), 2020*, pp. 1-6. doi: https://doi.org/10.23919/AEIT50178.2020.9241134.

41. Naboka B.G., Bezprozvannych A.V., Moscvitin E.S., Bytko M.V., Bytko S.M., Golovan A.A. Diagnostics of power system cable lines on dielectric dissipation factor and impregnated-paper insulation self-discharge time constant. *Electrical Engineering & Electromechanics.* 2011. no. 2. pp. 65-69. (Rus).

Received 14.09.2024
Accepted 14.11.2024
Published 02.03.2025

G.V. Bezprozvannych[1]*, Doctor of Technical Science, Professor,*
Y.S. Moskvitin[1]*, PhD,*
I.O. Kostiukov[1]*, Doctor of Technical Science, Assistant Professor,*
O.M. Grechko[1]*, PhD, Assistant Professor,*
[1] National Technical University «Kharkiv Polytechnic Institute», 2, Kyrpychova Str., Kharkiv, 61002, Ukraine,
e-mail: Hanna.Bezprozvannukh@khpi.edu.ua (Corresponding Author),
yevhen.moskvitin@khpi.edu.ua; ivan.kostiukov@khpi.edu.ua; a.m.grechko@gmail.com

How to cite this article:
Bezprozvannych G.V., Moskvitin Y.S., Kostiukov I.O., Grechko O.M. Dielectric parameters of phase and belt paper impregnated insulation of power cables. *Electrical Engineering & Electromechanics*, 2025, no. 2, pp. 69-78. doi: https://doi.org/10.20998/2074-272X.2025.2.09